Molecular Crystals and Liquid Crystals

Publication details, including instructions for authors and subscription information:
http://www.tandfonline.com/loi/gmcl20

On the Investigation of Field-Induced Director Dynamics: A Novel Esr Experiment

J. Becker [a], D. A. Dunmur [a], C. J. Dunn [a], G. R. Luckhurst [a], S. E. Marchant-Lane [a] & B. A. Timimi [a]

[a] Department of Chemistry and Southampton Liquid Crystal Institute, University of Southampton, Southampton, SO17 1BJ, United Kingdom

Version of record first published: 18 Oct 2010

To cite this article: J. Becker, D. A. Dunmur, C. J. Dunn, G. R. Luckhurst, S. E. Marchant-Lane & B. A. Timimi (2003): On the Investigation of Field-Induced Director Dynamics: A Novel Esr Experiment, Molecular Crystals and Liquid Crystals, 394:1, 45-61

To link to this article: http://dx.doi.org/10.1080/15421400390193666

Mol. Cryst. Liq. Cryst., Vol. 394, pp. 45–61, 2003

ISSN 1542-1406 print/1563-5287 online
DOI: 10.1080/15421400390193657

Taylor & Francis
Taylor & Francis Group

ON THE INVESTIGATION OF FIELD-INDUCED DIRECTOR DYNAMICS: A NOVEL ESR EXPERIMENT

J. Becker, D. A. Dunmur, C. J. Dunn, G. R. Luckhurst, S. E. Marchant-Lane, and B. A. Timimi*
Department of Chemistry and Southampton Liquid Crystal Institute, University of Southampton, Southampton, SO17 1BJ, United Kingdom

The rotational viscosity coefficient of a nematic liquid crystal with a positive diamagnetic susceptibility anisotropy can be determined by monitoring the time dependence of the director orientation as it is rotated by a field from a non-equilibrium to the equilibrium state parallel to the field. A variety of techniques is available using different properties to monitor the director orientation as a function of time. Normally these experiments are designed so that the property used to determine the director orientation does not change during the time taken for its measurement. Here using ESR spectroscopy, we explore the benefits of exploiting exactly the opposite situation. That is during the time taken to record the ESR spectrum the director orientation is allowed to change. We have developed both semi-quantitative and quantitative models to allow us to simulate how the form of the spectrum depends on experimental conditions such as the field scan rate. These models have also proved to be valuable in designing the experiment and in analysing the spectra. It seems that this novel ESR experiment provides a valuable route to the field-induced relaxation time and hence to the rotational viscosity coefficient.

Keywords: Nematic liquid crystals; rotational viscosity coefficient; field-induced relaxation time; ESR spectroscopy

1. INTRODUCTION

The response times of liquid crystal displays based on nematics are controlled by a variety of factors, but the rotational viscosity coefficient is of special importance [1]. As a consequence the determination of this

*Present address: Merck Specialty Chemicals Ltd., University Parkway, Chilworth Science Park, Chilworth, Southampton, SO16 7QD, United Kingdom.

We are grateful to Hitachi, the EPSRC (grant GR/H96904) and the TMR program (contract FMRX-CT97-0121) for their support of the research described in this paper.

viscosity coefficient has attracted considerable attention and a range of techniques is now available to do this [2]. Of particular value is a class of experiments in which the director orientation is changed by the application of an external magnetic or electric field. Then, provided the nematic director rotates as a monodomain, the relationship between the time dependence of the director orientation and the rotational viscosity coefficient is straightforward. Although several techniques can be used to determine the director orientation they do not all monitor the distribution in the director during alignment. However, magnetic resonance experiments, both NMR and ESR, allow the director distribution to be determined since the observed spectrum is usually a sum of spectra from all director orientations in the sample [3,4]. For the magnetic resonance experiment to be effective it is clearly desirable for the time taken to record the spectrum to be fast in comparison with the time taken by the director to change its orientation. For polymeric systems, such as the aramids, this is normally the case [5]. Indeed even for low molar mass materials this constraint is usually satisfied, except for NMR experiments where the high magnetic field of the spectrometer causes the rapid alignment of the director. In such experiments the time taken to measure the spectrum is essentially the effective spin-spin relaxation time during which the free induction decay tends to zero. When the director orientation changes during the free induction decay, for example in deuterium NMR experiments, the spectrum also contains small oscillations in addition to the anticipated quadrupolar doublet for a deuteron. The origin of these oscillations is understood and when they are observed their analysis in a single spectrum can result in the determination of the field-induced director relaxation time [6].

It is of considerable interest to see if analogous effects can be observed when ESR spectroscopy is used to determine the director orientation. We have already shown that ESR can be employed to give the instantaneous director orientation [4] by first determining the time dependent spectral intensity for a given field strength. By assembling these time decays into a matrix of time-field intensities it is possible to obtain conventional field sweep spectra at given times. Our aim now, however, is to see if we can acquire sufficient information to determine the field-induced relaxation time by scanning the magnetic field to record the spectrum in a time comparable to that required for the director orientation to change significantly. Here we describe the successful development of this novel ESR experiment for the investigation of field-induced director dynamics.

The layout of our paper is the following. In the next section we describe the theory necessary to simulate the ESR spectra during the field-sweep experiments. This theoretical background proved to be invaluable in designing both the experiments and analysing the results. The experiments are described in Section 3 and the results are given in section 4 where they

are discussed and compared with the theoretical predictions. Our conclusions are given in the final section.

2. BACKGROUND THEORY AND SPECTRAL SIMULATIONS

In order to simulate the ESR spectrum when the director orientation changes at the same time as the spectrum is recorded, we need to know the time dependence of the director orientation. This dependence is obtained by solving the torque-balance equation involving the magnetic and viscous torques, which gives [4,7]

$$\tan\theta(t) = \tan\theta_0 \exp(-t/\tau). \tag{1}$$

Here, θ_0 is used to denote $\theta(0^\circ)$, which is the initial director orientation with respect to the magnetic field and τ is the relaxation time

$$\tau = \mu_0\gamma_1/\Delta\tilde{\chi}B^2, \tag{2}$$

where μ_0 is the magnetic permeability of a vacuum, $\Delta\tilde{\chi}$ is the anisotropy in the magnetic susceptibility of the nematic, which is taken to be positive, B is the magnetic flux density and γ_1 is the rotational viscosity coefficient. To illustrate the time dependence of the director orientation we show $\theta(t)$ calculated from Eq. (1) with an initial orientation, θ_0, of 45° as a function of the scaled time, t^* $(=t/\tau)$. The results are given in Figure 1; we can see

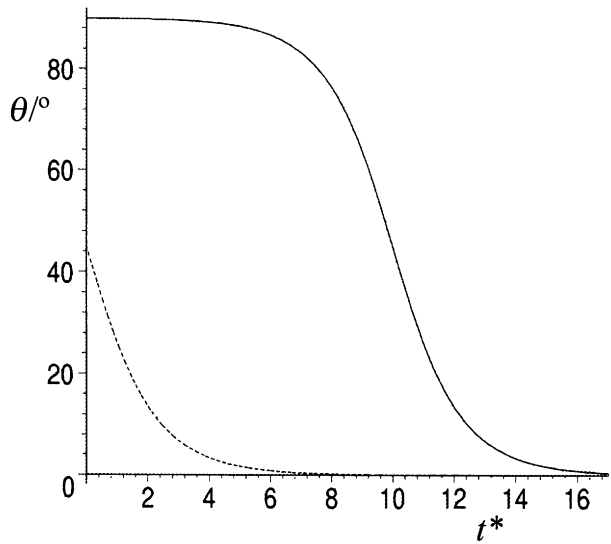

FIGURE 1 The dependence of the director orientation, θ, and the scaled time, t^*, calculated from Eq. (1) with $\theta_0 = 45^\circ$(-----) and $\theta_0 = 89.9^\circ$(——).

that the director orientation changes immediately and continuously until it reaches its limiting value of 0° when the director is aligned parallel to the magnetic field. It is of some interest to see how the decay process changes with the initial orientation of the director with respect to the magnetic field. To do this we take an extreme case with θ_0 equal to 89.9°; given the occurrence of $\tan\theta_0$ in Eq. (1) θ_0 clearly cannot be set equal to 90°. The results for $\theta(t)$, predicted by Eq. (1), as a function of the scaled time are also shown in Figure 1; they clearly differ significantly from the behaviour predicted with $\theta_0 = 45°$. Thus although the director orientation does change, the initial rate of change is extremely small, so much so that the results give the impression that there is a lengthy induction period for the alignment process. Following this there is a rapid change in the director orientation and then a slower return of the director to being parallel to the magnetic field.

We now turn to the background spectroscopy for the ESR experiment. Since the majority of nematogenic liquid crystals are diamagnetic they need to be doped with a paramagnetic spin probe if they are to be studied with ESR. The usual spin probes are organic nitroxides [8] in which the spin of the unpaired electron interacts predominantly with the spin of the nitrogen nucleus: as a consequence the ESR spectrum contains three nitrogen hyperfine lines. The two tensors, which determine the positions of the spectral lines, are the g tensor and the nitrogen hyperfine tensor, $\tilde{\boldsymbol{A}}$. In the fast motion limit the principal components of these partially averged tensors have the cylindrical symmetry of the nematic phase. The components parallel to the director are denoted by $\tilde{\boldsymbol{g}}_\parallel$ and $\tilde{\boldsymbol{A}}_\parallel$ while those perpendicular to the director are indicated by $\tilde{\boldsymbol{g}}_\perp$ and $\tilde{\boldsymbol{A}}_\perp$; as with other properties the tilde shows the value in the liquid crystal phase. In an ESR experiment the frequency, ν, is held fixed and the resonance condition is satisfied by scanning the magnetic field. The values of the resonance fields depend on the angle made by the director with the magnetic field, which is why ESR spectroscopy is such a powerful tool for the study of liquid crystals. The form of this angular dependence is given, in general, by [8]

$$\begin{aligned}\tilde{\boldsymbol{B}}_m(\theta) = {} & h\nu/\tilde{\boldsymbol{g}}\mu_B B - h\tilde{\boldsymbol{K}}m/\tilde{\boldsymbol{g}}\mu_B - (h^2\tilde{\boldsymbol{A}}_\perp/4\tilde{\boldsymbol{g}}^2\mu_B B^2) \\ & \times [(\tilde{\boldsymbol{A}}_\parallel^2 + \tilde{\boldsymbol{K}}^2)/\tilde{\boldsymbol{K}}^2][I(I+1) - m^2] \\ & - (h^2m^2/2\tilde{\boldsymbol{g}}^2\mu_B^2B^2)[(\tilde{\boldsymbol{A}}_\parallel^2 - \tilde{\boldsymbol{A}}_\perp^2)/\tilde{\boldsymbol{K}}]^2 \\ & \times (\tilde{\boldsymbol{g}}_\parallel^2\tilde{\boldsymbol{g}}_\perp^2/\tilde{\boldsymbol{g}}^4)\cos^2\theta\sin^2\theta; \end{aligned} \tag{3}$$

in this expression μ_B is the Bohr magneton, h is the Planck constant, I is the nuclear spin quantum number and m is the magnetic quantum number. The quantities $\tilde{\boldsymbol{K}}$ and $\tilde{\boldsymbol{g}}$ also depend on the director orientation according to

$$\tilde{g} = [\tilde{g}_\perp^2 + (\tilde{g}_\parallel^2 - \tilde{g}_\perp^2)\cos^2\theta]^{1/2} \tag{4}$$

and

$$\tilde{K} = [\tilde{A}_\perp^2\tilde{g}_\perp^2 + (\tilde{A}_\parallel^2\tilde{g}_\parallel^2 - \tilde{A}_\perp^2\tilde{g}_\perp^2)\cos^2\theta]^{1/2}/\tilde{g}. \tag{5}$$

In order to simplify our calculations and to make the basic physics of the experiment more apparent we shall make a number of approximations; these are valid for the nitroxide spin probe that is used in our experiments. The first is to ignore the second order correction terms represented by the last two terms on the right hand side of Eq. (3). This has the effect of making the hyperfine spacing between the first and second spectral lines equal to that between the second and third lines. The other approximation is that the anisotropy in the g tensor vanishes; that is that $\tilde{g}_\parallel = \tilde{g}_\perp$ which means that the central line in the spectrum for which $m = 0$ does not depend on the director orientation. With these approximations the resonance field in Eq. (3) becomes

$$\tilde{B}_m(\theta) = B_0 - (h/\tilde{g}\mu_B)[\tilde{A}_\perp^2 + (\tilde{A}_\parallel^2 - \tilde{A}_\perp^2)\cos^2\theta]^{1/2}m, \tag{6}$$

where the factor $h/\tilde{g}\mu_B$ converts the hyperfine tensor components which are in frequency units to field units.

We now use this expression together with Eq. (1) to calculate how the positions of the three hyperfine lines vary with time during the director rotation. To do this $\tilde{A}_\parallel$ and $\tilde{A}_\perp$ were assigned the values of 2.162MHz (7.70G) and 5.081MHz (18.10G), respectively, the scalar g factor was 2.0056 and the position of the central line was arbitrarily set equal to zero. The dependence of the angle between the director and the magnetic field on t^* was calculated from Eq. (1) with the initial director orientation, θ_0, set equal to 45°, as in the experiments which are described in the following section. The resulting line positions are shown as a function of the scaled time in Figure 2 where the horizontal axis gives the position of the resonance fields and the vertical axis is the scaled time. In the experiments the director is initially parallel to the magnetic field and so the nitrogen hyperfine spacing is $\tilde{A}_\parallel$ which is 7.70G. After the director has been rotated, essentially instantaneously, through 45° the hyperfine splitting has increased to about 14.9G, and then is seen to decrease as a function of time until it reaches its original value of $\tilde{A}_\parallel$, when the director is again parallel to the magnetic field. Although the outer two lines change their positions with time the central line remains fixed because of our assumption that $\tilde{g}_\parallel = \tilde{g}_\perp$ and that the second order terms are negligible (see Eqs. (3) and (4)). To record the ESR spectrum we now scan the magnetic field through the resonance fields: the field changes linearly with time and the straight lines in Figure 2 indicate how this field might vary. The particular form of the

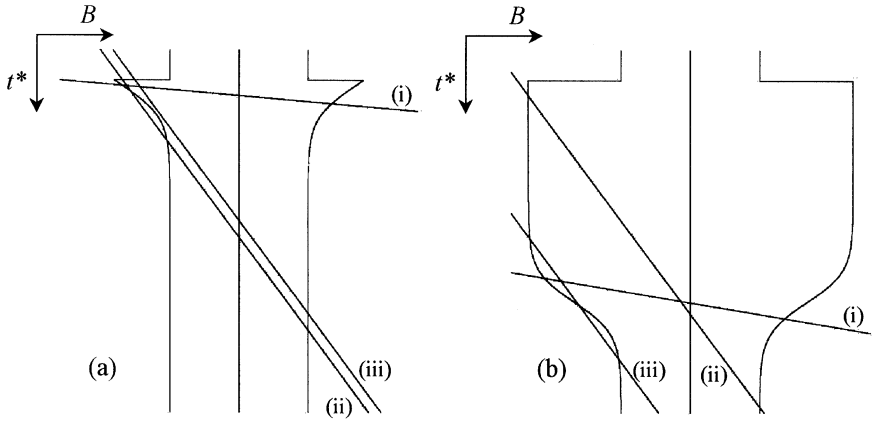

FIGURE 2 The dependence of the resonance fields for the three spectral lines on the scaled time, t^*, following the increase of the angle between the director and the magnetic field from 0° to (a) 45° and (b) 89.9°. The straight lines ((i)–(iii)) indicate a selection of scanning field profiles used to record the spectra.

time dependence is determined by the value of the magnetic field at which the director orientation is changed and the rate at which the field is scanned. More strictly it is the value of the magnetic field relative to that at which the central spectral line occurs which is of relevance. To see how these factors affect the spectrum which is recorded, we consider the calculated results for the 45° experiment, shown in Figure 2(a). For scan (i), which has the fastest rate, the line cuts each of the resonance field lines while the director orientation is still changing. The spectrum is predicted, therefore, to contain three hyperfine lines with unequal spacings. As we shall see these two hyperfine spacings will allow us to determine the field-induced relaxation time. For the scan corresponding to line (ii) the field changes at a much slower rate, and in addition the field at which the director orientation is changed is closer to the central field. As a consequence of the change in the scan profile, the field line cuts the $m = 1$ resonance field twice, the central resonance field ($m = 0$) once and the $m = -1$ resonance field once. The spectrum should, therefore, contain four hyperfine lines. In this case the spacings between the first three lines in the spectrum are unequal and they should be determined by the relaxation time, τ. In contrast by the time the final line is recorded the director has returned to being parallel to the magnetic field and so the hyperfine spacing is simply $\tilde{\boldsymbol{A}}_{\|}$ and contains no information about the director dynamics. The observation of four spectral lines for a nitroxide spin probe is clearly intriguing as is the final case which we consider for the 45° experiment.

The scan profile for this experiment is shown by line (iii) in Figure 2(a), it has the same slope as for the previous case but the initial field difference is slightly smaller. Now we see that this field does not cut the $m = 1$ resonance field but does for the other two ($m = 0$ and -1). It would seem, therefore, that the spectrum will contain just two lines and that the spacing between them would be $\tilde{A}_{\|}$, as in the previous example.

The analysis, which we have just presented, is based on the assumption that the spectral linewidth is zero. This assumption is clearly not true and so we now extend our discussion to include the finite width of the lines. We shall take the lineshape to be Gaussian largely as a result of inhomogeneous broadening caused by unresolved proton hyperfine structure [8]. The expression for the first derivative lineshape is

$$L(B, B_m, T_2) = (T_2^3/\sqrt{2}\pi)(B_m - B)\exp[-T_2^2(B_m - B)^2/2], \qquad (7)$$

where $2T_2^{-1}$ is the separation between the maximum and minimum peaks of the derivative lineshape. In addition, B_m is the resonance field (see Eq. (6)) and B is the field scanned to record the spectrum; in the experiments we have just described both of these fields vary with time. It is convenient to take the variable in the spectral simulations to be the field B. Given the field difference at the time origin and the slope, dB/dt^*, it is then possible to replace the scaled time by the field and hence determine the director orientation as a function of the field. This then allows the resonance fields also to be evaluated as a function of B. The results of these spectral simulations for the three 45° experiments are shown in Figure 3; the linewidth, $2T_2^{-1}$, was set equal to 0.6G which, as we shall see, is smaller than that of the nitroxide spin probe which we shall use in the real experiments but it does allow the variation in the spectra to be clearly discerned. The spectrum corresponding to the fastest scan rate is shown in Figure 3(i) and as we had anticipated it contains three hyperfine lines with unequal spacings. The second experiment with the slower scan rate which was predicted to give four spectral lines is shown in Figure 3(ii) and does indeed contain four hyperfine lines. The unequal spacings between these is clearly observed; however, what had not been anticipated was the reversal of phase for the spectral line for the lowest field. This occurs because unlike the other three lines B_m is smaller than B before the line centre at B_m is reached. As a consequence $(B_m - B)$ in Eq. (7) is, initially, negative and so a negative phase is observed. In the final 45° experiment we had expected just two lines to be observed but as the simulations demonstrate the spectrum contains three (see Fig. 3(iii)). The central and high field lines have the first derivative form which we have already seen but in contrast the unexpected line at low field has an unusual shape. It appears as an absorption lineshape, and not its derivative, but with a negative amplitude, as if in emission. In fact this shape is obtained because

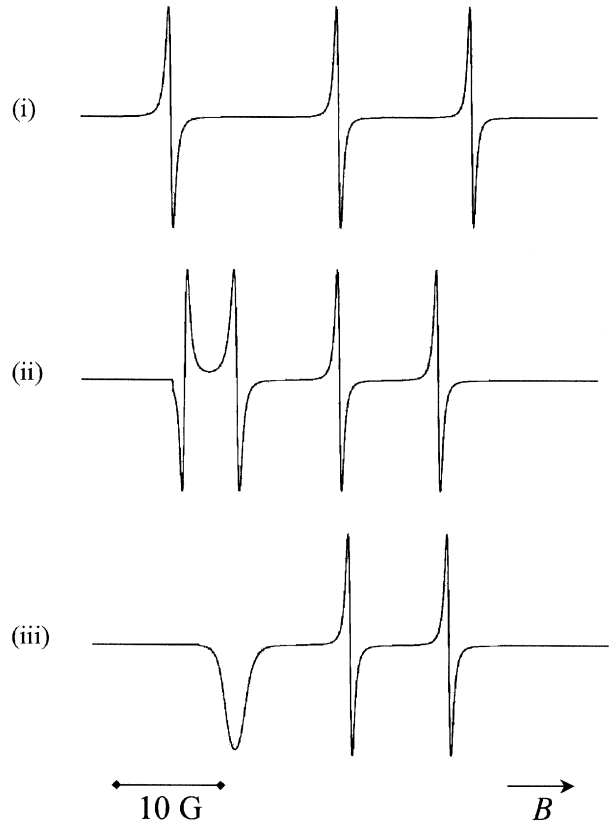

FIGURE 3 ESR spectra simulated for a nitroxide probe following the increase in the angle between the director and the magnetic field from 0° to 45° for the three scanning field profiles shown in Figure 2(a).

although the scanning field and the resonance field lines do not cross they approach sufficiently close that the negative region of the spectral line (see Fig. 3(iii)) is sampled by the scanning field. These simulations suggest that the ESR spectra recorded with a field scan time comparable to the time taken for the director reorientation to change should indeed exhibit some novel features from which aspects of the field-induced director dynamics could be deduced.

Before we turn to the experiments designed to test the ideas contained in these simulations, it is of interest to consider the extreme case when the field and director are initially, almost orthogonal to each other. The theoretical dependence of the three resonance fields on the scaled time is shown in Figure 2(b) and this clearly reveals the apparent induction

period. As a consequence of this period during which the hyperfine spacings do not change we consider three scan profiles different to those used in the 45° experiments. Profile (i) has the fastest scan rate and the largest initial field difference; this line cuts each of the resonance field lines just once and while the director orientation is still changing. As a consequence the spectrum contains three hyperfine lines with unequal spacings. Profile (ii) has a much smaller slope and a lower initial field; this cuts the $m = 1$ resonance field line before the director orientation has changed to any significant extent and the $m = -1$ resonance field line after the director has returned to being parallel to the magnetic field. The spectrum will also contain three resonance lines with hyperfine spacings, $\tilde{A}_{\perp}$ and $\tilde{A}_{\parallel}$, corresponding to the maximum difference between them. However, this limiting spectrum contains no quantitative information about the field-induced director dynamics. The third scan profile (iii) has the same slope as the second but with a significantly lower initial field difference. With this particular selection of parameters the scanning field cuts the $m = 1$ resonance field three times as the change in the director orientation causes this to vary. Subsequently the $m = 0$ and $m = -1$ resonance field lines are cut just once after the director is again parallel to the magnetic field, although this is not shown in Figure 2(b). The spectrum should then contain five hyperfine lines and the spacings between those in the low field region of the spectrum will relate directly to the field-induced director dynamics. In practise, however, we expect that the spectrum might be even more complex because when the field is initially orthogonal to the director there is a degeneracy in the alignment pathway. One important consequence of this is that the nematic does not move as a monodomain during the alignment process [9]. The ESR spectrum will, therefore, be a powder pattern formed by the weighted sum of spectra from each director orientation. The analysis of such spectra is complicated because there is not a simple expression for the spatial and temporal distribution of the director. We shall not, therefore, pursue the form that the spectrum might take when the field and director orientation change at the same rate any further here.

3. EXPERIMENTAL

The nematic liquid crystal used to explore our ideas for this novel ESR experiment was the commercial material ZLI-4792 which is available from Merck and is a mixture of fluorinated compounds. This particular nematic was chosen because its dynamic behaviour has been well-studied with ESR spectroscopy [4,10]. In addition it has a long nematic range, and at room temperature, where our measurements are made, the orientational order is high so that the anisotropy in $\tilde{A}$ is large which facilitates the ESR

experiments. The cholestane spin probe ((3-spiro-[2′-N-oxyl-3′, 3′-dimethyloxazolidine])-5-α-cholestane was used because its large length-to-breadth ratio also helps to enhance the anisotropy in $\tilde{\boldsymbol{A}}$. The concentration of the cholestane spin probe in ZLI-4792 was approximately 1×10^{-2}wt% which gives a good signal-to-noise ratio without causing any concentration broadening of the spectral lines. The sample was placed in a 4 mm internal diameter pyrex tube, and was degassed to remove dissolved oxygen which can also broaden the lines. The sample tube was placed in the TE_{102} microwave cavity of a Bruker ECS 106 spectrometer. The tube was connected, through a flexible coupling, to a rotary solenoid (Radio Spares; 439-997, rotation angle 45°) which was used to rotate the sample tube and hence the director [4] in order to change the angle between the director and the magnetic field from 0° to 45°. This is necessary because it is not possible to change the orientation of the magnetic field with this ESR spectrometer.

In these experiments the scan range was fixed at 50G which covers the spectral width for this particular spin probe in ZLI-4792 at room temperature. Following the initiation of the scan the rotary solenoid was activated to change the director orientation more or less instantaneously. The maximum time difference between starting the scan and rotating the director which could be used was 0.5 s. Since this time controls the initial value of the field it would be useful to be able to increase this value. However, this is not possible and instead we have found it valuable to be able to vary the position of the central spectral line with respect to the field at the moment when the director is rotated. The remaining parameter is the scan time which controls the rate at which the field is changed. The smallest scan time available that gives a spectrum with a good signal-to-noise ratio is 1.31 s and this can only be increased in powers of two, which again limits the range of experiments which we are able to perform with this particular ESR spectrometer. In the experiments which we report here the scan time was fixed at 5.24 s.

4. RESULTS AND DISCUSSION

In the first experiment we sought to obtain a spectrum with three hyperfine lines with unequal spacings. To do this, the separation between the central field and the initial field was 21.75 G and the scan time was 5.24 s corresponding to a scan rate of $9.54\,\mathrm{Gs}^{-1}$. The resultant spectrum is shown in Figure 4(a) and clearly contains three unequally spaced hyperfine lines. The spacing separating the high field line from the central peak is 8.28G. This value is greater than that of 7.61G measured for $\tilde{\boldsymbol{A}}_{\|}$ from the static spectrum and shows that the director has not been aligned parallel to

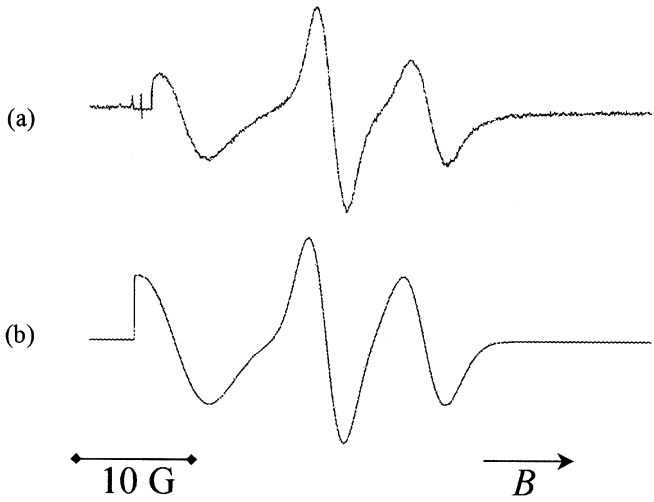

FIGURE 4 The ESR spectrum of the cholestane nitroxide spin probe dissolved in the nematic host ZLI-4792 following the rotation of the director by 45° (a) measured with the conditions described in the text and (b) simulated via Eqs. (1), (6) and (7) using the parameters given in the text.

the magnetic field when the high field line was recorded. The low field line is clearly incomplete and results from the fact that the scanning field has reached a value close to the centre of the low field line after the director had been rotated by 45°. The other spectral features which should be noted relate to the linewidths. First, they are significantly broader than those used in the spectral simulations shown in Figure 3, and secondly the widths of the three lines are not quite the same, although this differential broadening in an anisotropic environment is well-understood [11]. To show that the real spectrum is well-accounted for by the theory which we have developed, we have simulated the spectrum with $B_0 - B(0)$ of 21.75 G, τ of 1.46 s and the three linewidths 3.8G ($m = 1$), 3.0 G ($m = 0$) and 3.8 G ($m = -1$). The simulation is shown in Figure 4(b) and is clearly in good but not perfect agreement with the experiment. The line positions are in quantitative agreement with experiment which convinces us that we can estimate the field-induced relaxation time, τ, from the hyperfine spacings. Since, to a good approximation, the central line position does not depend on the director orientation, the hyperfine spacing associated with the low field line gives, via Eq. (6), the director orientation at time t_1. This time is determined from the scan rate and the field position of the low field line relative to the field value at which the director was rotated. Similarly the

hyperfine spacing associated with the high field line gives the director orientation at time t_2, which is again evaluated from the field position of the high field line. Each of these director orientations could, with a knowledge of t_1 and t_2, together with the initial director orientation be used to estimate two values for the field-induced relaxation times from Eq. (1). In practise, however, it is difficult to determine the time at which the director orientation is changed and the rotation angle with sufficient accuracy. Fortunately, we can solve both problems by taking the ratio of the tangents of the two angles, which gives

$$\tan\beta_1/\tan\beta_2 = \exp[-(t_1 - t_2)/\tau]. \tag{8}$$

This is conventionally written in terms of the two hyperfine splittings, α_1 and $\tilde{\boldsymbol{a}}_2$; rearrangement of the equation then gives the relaxation time as

$$\tau = 2(\tilde{\boldsymbol{a}}_1 + \tilde{\boldsymbol{a}}_2)/b \ln[(\tilde{\boldsymbol{a}}_1^2 - \tilde{\boldsymbol{A}}_\parallel^2)(\tilde{\boldsymbol{A}}_\perp^2 - \tilde{\boldsymbol{a}}_1^2)/(\tilde{\boldsymbol{A}}_\perp^2 - \tilde{\boldsymbol{a}}_1^2)(\tilde{\boldsymbol{a}}_2^2 - \tilde{\boldsymbol{A}}_\parallel^2)], \tag{9}$$

where b is the rate at which the field is scanned ($b = 9.54\,\mathrm{Gs}^{-1}$). In order to estimate the experimental error in the relaxation time determined in this manner from the two hyperfine splittings we have repeated the experiment ten times. This gives τ for ZLI-4792 at room temperature ($\sim$20°C) as 1.44 ± 0.09s, which is in very close agreement with the value of 1.42 s determined from a complete set of time-resolved ESR spectra [10]. The error in this new determination is approximately 6%, which is necessarily higher than that, 1%, resulting from the use of a dramatically larger data set. The error in the value of τ determined from the single spectrum clearly depends on how close the director is to being aligned parallel to the magnetic field when the low and high spectral lines are measured. Assuming that the error in measuring the hyperfine spacing is 0.1G, although it can be somewhat smaller than this, the error in τ is found to be in the range 4–6% provided the hyperfine spacing, $\tilde{\boldsymbol{a}}_2$, is greater than $\tilde{\boldsymbol{A}}_\parallel$ by about 0.6G. This error in τ does not seem to be unreasonably high in comparison with other methods, and this new ESR technique certainly has the advantage of being rapid.

The other aim of our experiments was to verify the predictions of the unusual spectral features made by the analysis presented in section 2. To do this we have performed a series of experiments in which the rate at which the magnetic field is changed is held constant at $1.192\,\mathrm{Gs}^{-1}$ but the difference between the field value when the director is rotated and the field at the central line is varied. The experimental spectra for the cholestane spin probe dissolved in ZLI-4792 for a selection of field differences are shown in Figure 5(i). To appreciate these experiments and their results we show in Figure 5(ii) the field plots with the resonance fields calculated

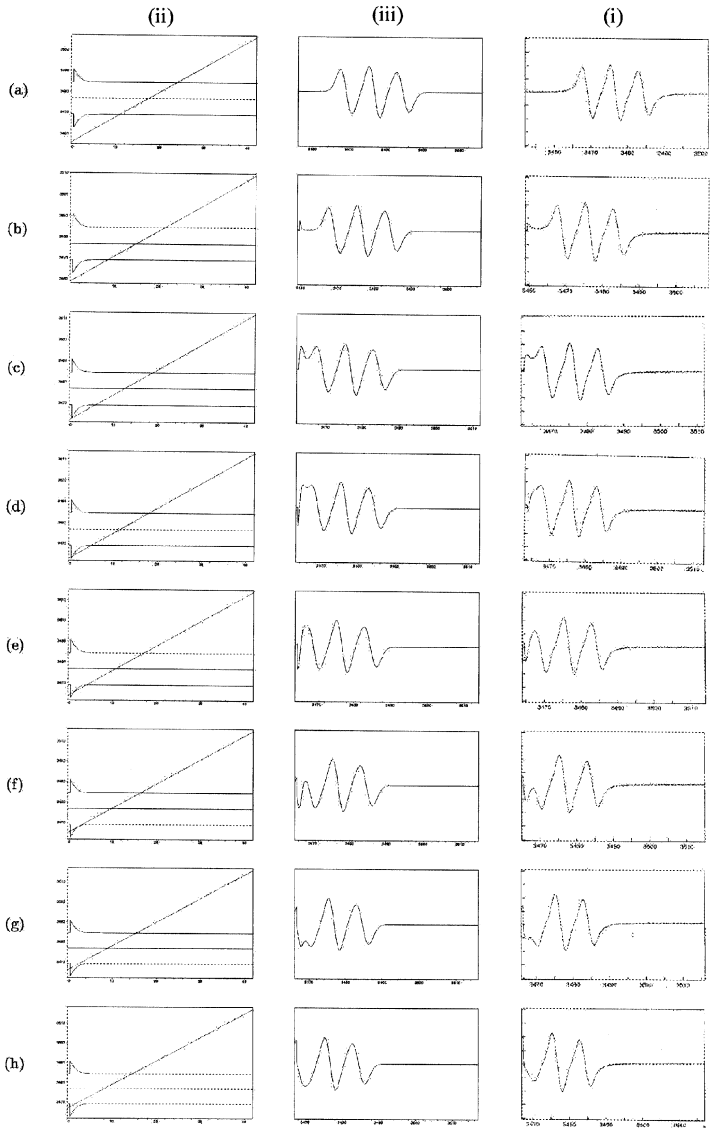

FIGURE 5 (i). The experimental ESR spectra of the cholestane spin probe recorded after the rotation of the director by 45° for the nematic ZLI-4792 for a series of scan profiles differing in the initial field relative to that for the central peak. To understand the nature of the spectra and their variation we show the time dependence of the resonance lines together with the scan profiles with their differing initial field values in (ii). The simulated spectra obtained for the various scan profiles are shown in (iii). The horizontal axes in Figures (i) and (iii) are in gauss and in Figure (ii) is in seconds.

using the same parameters as those used to construct Figure 2(a). The first scan profile shown in Figure 5(ii,a) has the largest field difference and so the scanning field cuts all three resonance fields after the director has returned to being parallel to the magnetic field. The spectrum is expected to contain three hyperfine lines with both spacings equal to $\tilde{A}_{\|}$; this is certainly the case as the experimental spectrum shows (see Fig. 5(i, a)). In Figure 5(ii, b) the field difference has decreased and so the scanning field first approaches the $m=1$ resonance field before cutting it after the director is once more parallel to the magnetic field. We expect, therefore, that the spectrum will again contain three hyperfine lines with two equal spacings of $\tilde{A}_{\|}$. However, there might also be an initial spectral line with an unusual shape depending on the width of the low field line. This feature is indeed observed in the experimental spectrum as a decaying tail just after the start of the scan, together with the three equally spaced hyperfine lines (see Fig. 5(i, b)). As the field difference is further reduced, so the scanning field approaches more closely to the initial stage of the $m=1$ resonance field (see Fig. 5(ii, c)). We expect, therefore, to see a stronger feature in the spectrum before the normal three line spectrum appears, and this proves to be the case (see Fig. 5(i, c)). In addition, the extra spectral feature has become closer to the low field line, as we might have anticipated from the field plot in Figure 5(ii, c). The next reduction in the field difference now causes the scanning field to cut the resonance field for $m=1$ twice (see Fig. 5(ii, d)). We expect, therefore, to see an additional hyperfine line at low field but with the opposite phase to that for the other three spectral lines. The extra line is clearly apparent in the experimental spectrum but not all of the line is observed, partly because the large linewidths cause the spectral lines to overlap. In addition, the difference between the scanning field and the resonance field does not become sufficiently small in comparison with the linewidth, for the entire lineshape to be observed (see Eq. (7)). As the field difference is decreased further, so the fields at which the scanning field cuts the $m=1$ resonance field become more similar (see Fig. 5(ii, e)), and because of the large linewidth the two lines which should be observed at low field merge into a single peak (see Fig. 5(i, e)). However, the opposite phases of the two peaks means that there is a reduction in the overall line intensity and a negative region at the start of the spectrum. This behaviour is more apparent for the experimental spectrum shown in Figure 5(i, f) where the low field peak is very small and has an unusual shape. The reason for this behaviour is clearly apparent from the associated field plot in Figure 5(ii, f) where the scanning field is essentially tangential to the $m=1$ resonance field curve; that is the points at which the lines intersect are virtually identical. Further decrease in the field difference means that the scanning field does not intersect the $m=1$ resonance line (see Fig. 5(ii, g)). The low field line should then

vanish but because the two fields approach within a distance comparable to the linewidth, a spectral feature is observed at low field (see Fig. 5(i, g)). In the final experiment the field difference has been decreased further still so that the scanning field does not pass so close to the $m = 1$ resonance field. The difference between these fields, $(B_m - B)$, is always negative (see Fig. 5(ii, h)) and so this contributes an emission-like feature to the spectrum (see Figs. 3(iii) and 5(i, h)). The experimental spectrum also shows a positive intensity for a small field range at the very beginning of the scan. This is also apparent in the other spectra (see, for example, Figs. 5(i, d)–(i, h)), although the intensity decreases as the field difference between the initial field and the field at the central line increases. This feature originates from the low field spectral line before the director orientation changes. As the scan profiles in Figures 5(ii, a)–(ii, h) show, the scanning field approaches closer to the $m = 1$ resonance field in this sequence and so the spectral intensity also increases.

As we have seen both here and in section 2, the scan profiles provide an excellent means of designing the experiment and in understanding the essential features of the spectrum obtained. However, they do not provide a quantitative interpretation of the observed spectra. To achieve this it is necessary to simulate the spectra allowing for the finite linewidths and the differential line broadening. We have, therefore, used the approach described in section 2 to simulate the series of spectra, which we have measured as a function of the field difference between the initial field and the field value for the central line. In these simulations the spectral parameters were kept at the values introduced in section 2 with the rate of change of the field equal to the experimental value of $1.192 \mathrm{Gs}^{-1}$ and the field-induced relaxation time equal to 1.40s, which is close to the value obtained experimentally. The only variable in the simulations was the field difference, and the values used were taken from the experimental parameters. The overall agreement between the simulations (see Fig. 5(iii)) and the experimental spectra (see Fig. 5(ii)) is seen to be excellent. Of particular importance is the comparison in the low field region where the director dynamics have the greatest influence. Indeed in this series of experiments, the dominant hyperfine lines are associated with the director after it has returned to being parallel to the magnetic field. The features of the low field spectral region are surprisingly well-accounted for by the simulation, although the intensities are not perfectly reproduced. This may result from the variation of the linewidths with the director orientation [11], which has not been allowed for in the simulations. Notwithstanding this minor mismatch, the agreement in this spectral region indicates that the model we have developed to simulate the spectra is reliable, and can be used with confidence to extract the field-induced relaxation time from the experimental spectra.

5. CONCLUSIONS

We have demonstrated that ESR spectroscopy can be employed to determine the relaxation time for the field-induced director alignment from a single spectrum. To achieve this, it is necessary to set the magnetic field following the initial change in the director orientation together with the rate at which the field is changed so that the director is still being aligned by the field during the time that the spectrum is recorded. A range of experiments is possible by varying the field difference and the rate at which the magnetic field is changed. The simplest situation occurs when the director has not been aligned by the time that the high field line is recorded and the low field line is observed almost immediately following the change in the director orientation. Then for a nitroxide spin probe the two hyperfine spacings are unequal and the field-induced director relaxation time can be obtained directly from these, quickly and with reasonable accuracy. However, even when the rate at which the field is scanned is slower, so that the director has returned to being parallel to the field by the time the high field line is recorded, new spectral features are found in the low field region of the spectrum, which do depend on the field-induced director dynamics. This information can be extracted from the spectrum by simulating it and optimising the match between the experimental and simulated spectra. The methodology which we have developed here complements the method where time-resolved ESR spectra are obtained indirectly for the period taken for the director to be aligned parallel to the magnetic field. This detailed experiment clearly provides more information not only to determine the field-induced relaxation time but also to ensure that the relaxation process is correctly predicted by the solution of the torque-balance equation. The new methodology has the advantage that it is fast and so can be used to screen a large number of systems under a variety of conditions.

REFERENCES

[1] Schadt, M. (1994). In: *Topics in Physical Chemistry: Liquid Crystals*, H. Stegemeyer. (Ed.), Steinkopff, Darmstadt; Springer: New York, Vol. 3, Chap. 6.
[2] Moscicki, J. K. (2001). In: *Physical Properties of Liquid Crystals: Nematics*, Dunmur, D. A. Fukuda, A, & Luckhurst, G. R. (Eds.), INSPEC London, Chap. 8.2.
[3] Dunn, C. J., Luckhurst, G. R., Miyamoto, T., Naito, H., Sugimura, A., & Timimi, B. A. (2000). *Mol. Cryst. Liq. Cryst., A*, *347*, 167.
[4] Dunn, C. J., Ionescu, D., Kunimatsu, N., Luckhurst, G. R., Orian, L., & Polimeno, A. (2000). *J. Phys. Chem. B*, *104*, 10989.
[5] Fan, S. M., Luckhurst, G. R., & Picken, S. J. (1994). *J. Chem. Phys.*, *101*, 3255.
[6] Kantola, A., Luckhurst, G. R., Sugimura, A., & Timimi, B. A. (2003). *Mol. Cryst. Liq. Cryst. A*, in the press.

[7] Wise, R. A., Olah, A., & Doane, J. W. (1975). ***J. Phys. (Paris)***, ***36***, C1, 117.
[8] Luckhurst, G. R. (1974). In: ***Liquid Crystals and Plastic Crystals***, Gray, G. W. & Winsor P. A. (Eds.), Ellis Hordwood Ltd: Chichester, Vol. 2, Chap. 7.
[9] Esnault, P., Casquilho, J. P., Volino, F., Martins, A. F., & Blumstein, A. (1990). ***Liq. Cryst.***, ***7***, 607.
[10] Kunimatsu, N. (2000). Ph.D. Thesis, University of Southampton.
[11] Luckhurst, G. R. & Sanson, A. (1972). ***Mol. Phys. 24***, 1297.